

A numerical simulation of impact force on a heaved floating body with moving boundaries

A.A.A. Moustafa

Dept. of Eng. Mathematics and Physics, Faculty of Eng., Alexandria University, Alexandria, Egypt

A numerical model based on the Boundary Integral Method (BIM) is presented for solving the impact problem of a general two-dimensional bluff body striking a water surface. The model solves the potential flow equation, including the full nonlinear kinematic and dynamic free surface boundary conditions. The numerical procedures are applied to predict the wave field generated by heaving wedge-shaped bodies with varying wedge angles and heaving amplitudes. The choice of the wedge shape has been commented upon and its reasons are given. A series of sensitivity study cases were performed to investigate the computational characteristics of the model. Simulations are performed for various parameters which govern the motion of an oscillating body. Numerical results were compared with available experimental data, and a qualitative agreement is achieved.

يتم البحث نمودجا عدديا لحساب أحمال الارتطام على أسطح الأجسام العائمة نتيجة لحركة تلك الأجسام حركة تردديه في الاتجاه الراسي نظرا لحركة سطح الجسم العائم وكذلك حركة السطح الحر لمياه المجرى الملاحي لذا اعتمد النمودج المقترح على اجراء الحسابات المطلوبة من خلال مرحلتين متتابعين الأولى لحساب الموضع الجديد للأسطح المتحركة والثانية لحساب أحمال الارتطام على تلك الأسطح في الوضع المحسوب من الخطوة الأولى كما قدم البحث علاجاً للتحكم في حسابات ظاهرة اندفاع المياه على اثر ارتطامها بسطح الجسم العائم خاصة في حالة وجود روايا ميل كبيرة لهذا السطح. وقد تم استخدام النمودج المقترح في حل مسائل الأجسام ذات القطاع المثلث على الرغم من صلاحية النمودج لدراسة كافة أنواع الأسطح الا ان اختيار القطاع المثلث قد تم بناء على ان هذا القطاع يمثل النواة الأساسية لوحدة بناء وتكوين كافة القطاعات المشكلة لبس السفينة وخاصة الشكل العام لمقطع مقدمة السفينة ذلك المقطع الأكثر تعرضا لهذه الأحمال على طول المحور الطولي للسفينة وأيضا لتوافر النتائج العملية لهذا المقطع (لدارسين اخرين) وقد ساهمت تلك النتائج في الحكم على درجة الدقة للنمودج المقترح من خلال مقارنة النتائج وبوه البحث إلى وجود بعض الاختلافات في النتائج ويبس سبب القصور ه اقتراحات سبل العلاج في در اسباب لاحقه

Keywords: Slamming, Numerical simulation, Impact force, Heaved floating body

1. Introduction

One of the complex problems, which have been addressed in hydrodynamics, is the impact problem. The problem arises in ocean-going vessels or fast boats when the hull impacts the free surface. This slamming load can result in substantial damage in the structures of ship hull and marine facilities. Owing to its practical importance in ocean engineering, the water-body impact problem has attracted a large number of investigators. The impact problem first emerged in the stress analysis of seaplane landings by the approximations of Von Karman [1] and Wagner [2], these approximations became the basic reference for many subsequent investigators. Early studies concentrated on predicting first-order behavior for simple heaving motion [3],

this was extended to include second-order effects and other body motions [4,5,6]. Lee [7] developed a series of second-order theories based on expansion of non-dimensionalized heaving amplitude.

With the advent of computers, it becomes possible to study the impact problem much more effectively. Computer calculations allowed the investigators to analyze nonlinear effects by simulation. In an effort to solve the nonlinear free surface problem, Chapman [8], developed a numerical two-dimensional flow induced by the motion of a floating body. Greenhow [9], presented a numerical solution to the impact problem based on the Cauchy's theorem to calculate the complex potential and its derivatives along the boundary. Dommermuth [10] and Pukhnachov [11] developed a numerical method for nonlinear three-dimensional

axisymmetric free surface problem using a mixed Eulerian-Lagrangian Scheme.

A Finite-Difference Method (FDM), with a modified Euler method for the time domain was used by Howison [12] Spaulding [13] to predict the wave field generated by heaving floating bodies. The FDM is most suitable method for rectilinear boundary on the free surface. The principal deficiency of FDM, when applied for the problem in hand, is its inability to follow the moving boundaries easily. The Finite Element Method (FEM) has flourished in the field of complicated geometry. The FEM requires that, the problem to be solved is in a variation form. A large number of investigations [14-17] used the FEM for modeling wedge-shaped bodies with varying wedge angles and heaving amplitudes. With complex shaped bodies as well as the free surface configurations, the need for the boundary fitted coordinate becomes essential for better simulations. Wang and Spaulding [18] introduced a two-dimensional potential flow for a general body configurations in heaving motion. Mei and Dick [19] provided an approach using the body fitted coordinate system for the complex geometrical bodies with a free surface.

When the impact problem is solved using numerical calculations, there are a number of difficulties to cope with, some of which are the accumulation of the numerical error and memory limitation. The accumulation of the numerical error can cause serious error, which contaminate the numerical results, or cause the results to diverge. This is defined loosely as numerical instability. To prevent this numerical instability, numerical schemes should be chosen carefully and operated within a proper parametric range. The stability criteria of some numerical schemes were derived [20,21] to overcome the divergence of the results.

Many investigators treated the impact problem analytically. Alexander [22], has derived an analytical method based on the hypothesis that the impact velocity is equal to the relative velocity normal to the impact surface of the moving body. More recently, Wu. [23] developed analytical forms of the

nonlinear hydrodynamic force on a floating body.

Several methods for solving the governing equations of the impact problem with moving boundaries discussed in [24,25], and the typical one used in this study, is the two-step approach with moving boundaries. In the two steps approach, the governing equation is solved first on a temporarily fixed boundary, and then the free surface boundary equations are solved to determine the new boundary position and the values of the normal derivatives on that boundary. These two steps are iterated as a function of time, each step can be solved in the Eulerian sense, where all the physical values are calculated at the spatial points, or in the Lagrangian sense, where all the physical values are calculated along the path of the moving water particles. The goal of the present study is to apply a numerical model to predict the impact force on a heaved body when nonlinear free surface dynamic boundary effects are important.

2. Formulation of the problem and governing equations

Consider an infinitely long two dimensional symmetrical body which is forced to oscillate vertically on a free surface. For the time being the body shape may be assumed to be arbitrary and the body motion can be cyclic or linear with constant velocity in the y -direction, while the free surface is given by:

$$\psi(\bar{x}, t) = 0, \quad (1)$$

where $\bar{x} = \bar{x}(x, y)$ is the position vector in the right hand coordinate system. The y -axis is defined to be positive in the upward direction, while the x -axis represents the calm water level. The origin is at the intersection of the vertical centerline of the body and the undisturbed water surface. fig. 1 depicts the above-described setup. The fluid is assumed to be incompressible, inviscid, and the flow is assumed to be irrotational. Based on the above assumptions, a velocity potential $\phi(\bar{x}, t)$ can

be introduced, and the velocity vector of a fluid particle is given by;

$$\bar{u} = \nabla\phi. \tag{2}$$

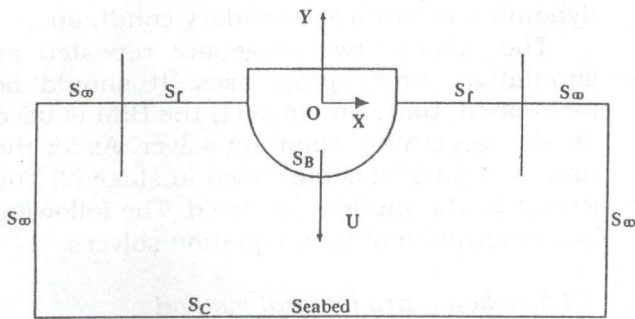


Fig. 1. Coordinates and geometry of the free surface problem.

Furthermore, the effect of surface tension at the free surface is neglected, and water depth is assumed to be deep enough allowing the bottom (sea-bed), effect to be ignored. The water surface is assumed to start from rest. Following the above assumptions the mathematical model describing the problem under investigation is based on the conservation of mass principle.

It is well accepted that, inside the fluid domain, mass is neither created nor destroyed. Thus, this statement is expressed mathematically by the Laplace equation, in the fluid domain, namely;

$$\nabla^2 \phi = 0. \tag{3}$$

In order to solve the impact problem, Laplace equation must satisfy the following boundary conditions:

1. *The kinematics free surface boundary condition.* This condition is applied on the free surface and it expresses the fact that, the normal velocity of the water particle on that free surface is the same as the normal velocity of the free surface itself. In other words, once a particle is on the free surface, it remains there, this kinematic boundary condition can be written as:

$$\frac{D(y - \eta)}{Dt} = \frac{\partial}{\partial t} (y - \eta) + \nabla\phi \cdot \nabla (y - \eta) \text{ on } y = \eta(x, y), \tag{4}$$

where, D/Dt denotes the substantial or material derivative. This condition is used to follow the free surface as a function of time.

2. *Dynamic free surface boundary condition.* Based on Bernoulli's equation, it is assumed that, the pressure on the free surface must be atmospheric. Thus such condition is expressed as;

$$\frac{P}{\rho} + \frac{\partial\phi}{\partial t} + \frac{1}{2} \left[\left(\frac{\partial\phi}{\partial x} \right)^2 + \left(\frac{\partial\phi}{\partial y} \right)^2 \right] + gy = 0. \tag{5}$$

Where,

P is the pressure, and ρ is the fluid density.

The above condition at $y = \eta(x, y)$ becomes:

$$\frac{D\phi}{Dt} = -g\eta + \frac{1}{2} \nabla\phi \cdot \nabla\phi. \tag{6}$$

This condition is to be used to determine the value of the potential on the free surface.

3. *Body Boundary Condition.* This condition states that, a fluid particle cannot penetrate the solid body surface but rather it stays in direct contact with this surface. Hence, the normal velocity of the particle on the body surface is the same as that of the body surface itself. Mathematically, this condition is expressed as;

$$\bar{U} \cdot \bar{n} = \nabla\phi \cdot \bar{n}. \tag{7}$$

The above condition is applied on the body surface whose equation is;

$$S_B(x, y, t) = 0. \tag{8}$$

Where,

\bar{U} is the body velocity,

$\nabla\phi$ is the fluid particle velocity vector on the body,

\bar{n} is the unit normal vector directed outwards from the domain of the interest and into the body, and

S_B is the body surface (see fig. 1).

4. *Far field condition.* Since the field occupied by the water is unbounded, the far field

condition states that, the normal velocity far away is assumed to tend to zero, hence we can write;

$$\frac{\partial \phi}{\partial n} \rightarrow 0 \text{ as } |r| \rightarrow \infty, \quad (9)$$

where $|r|$ is the distance from the origin.

In practice the term far away is taken as a long distance from the origin, and thus special care must be exercised during computational procedures.

3. Solution procedure

Before such procedure is discussed, it is worth mentioning that numerical simulation is adopted as a method for solution. Furthermore, simulation times are taken short enough so that no significant waves generated by the body have to be propagated into the far field boundary S_∞ . Such simulation times, however, allow the computation of the physical quantities of interest, mainly, the potential values, and the pressure on the body during impact as well as the position of the free surface. There are a number of methods to solve the Laplace equation and the accompanying boundary conditions. In the present work the following procedure is implemented.

Stage (1): A temporarily fixed boundary is assumed. The governing Laplace equation is solved on that boundary using the Boundary Integral Method (BIM). The BIM uses the information (the potential values or the derivatives of the potential) only and on the boundary. In the impact problem, either the potential values are given (a Dirichlet boundary condition) and the normal derivatives of the potential values are unknown on the free surface. While, the normal derivatives are known and the potential values are unknown on the body (a Neumann boundary condition). Thus the values of the velocity potential obtained; hence the values of the normal derivatives of ϕ being calculated.

Stage (2): Using the free surface boundary conditions one can locate the new position of the free potential at such new location, Thus

applying the kinematic free surface boundary condition we get the new location of the free surface. Subsequently on the new free surface, one can determine the up-dated values of the velocity potential using the dynamic free surface boundary condition.

The above two stage are repeated as simulation time progresses. It should be mentioned that, in stage (1) the BIM is used as the governing equation solver. As for the time stepping scheme used in stage (2) The Runge-Kutta method is used. The following is a description of both equation solvers.

3.1. The boundary integral method

The mathematical formulation for the Boundary Integral Method (BIM) begins with the divergence theorem;

$$\iiint \nabla \cdot \bar{U} \, dV = \iint \bar{n} \cdot \bar{U} \, ds. \quad (10)$$

Where,

\bar{U} Is the fluid velocity vector that is continuous and differentiable in the domain (V), and

\bar{n} Is the outward normal vector.

This theorem states that, the total increase of the volume of fluid is the same as the total flux through the surface. The divergence theorem is applied to Green's first identity.

$$\nabla \cdot (G \nabla \phi) = G \nabla^2 \phi + \nabla G \cdot \nabla \phi, \quad (11)$$

hence, produces the integral equation, Green's second identity.

$$\iiint (\phi \nabla^2 G - G \nabla^2 \phi) \, dV = \iint \left(\phi \frac{\partial G}{\partial n} - G \frac{\partial \phi}{\partial n} \right) \, ds. \quad (12)$$

The above volume integrals are taken over the fluid domain, while the surface integrals are taken over its surrounding surfaces.

In two dimensions, the volume integral becomes a surface integral and the surface integral becomes a line integral. The fluid domain of the interest V is surrounded by a body surface S_B , free surface S_f , free

surface at infinity S_∞ , and the other far-field contour including bottom S_c (see fig. 1).

Two quantities are introduced in eq. (12), ϕ is defined as the velocity potential which satisfies Laplace's equation and G as the solution of the Poisson equation. the fluid domain;

$$\nabla^2 \phi = 0,$$

and

$$\nabla^2 G(\bar{x}; \bar{\zeta}) = -\delta(\bar{x} - \bar{\zeta}) = -\frac{\delta(\bar{r})}{2\pi r}. \quad (13)$$

Another solution G^* can be obtained by adding any analytic homogeneous solution to the particular solution, as follows;

$$G(\bar{x}; \bar{\zeta}) = -\frac{1}{2\pi} \ln |\bar{x} - \bar{\zeta}| = -\frac{1}{2\pi} \ln r, \quad (14)$$

$$G^*(\bar{x}; \bar{\zeta}) = -\frac{1}{2\pi} (\ln r + \ln c) = -\frac{1}{2\pi} \ln rc, \quad (15)$$

and

$$\nabla G(\bar{x}; \bar{\zeta}) = \frac{1}{2\pi} \frac{(\bar{x} - \bar{\zeta})}{|\bar{x} - \bar{\zeta}|^2}. \quad (16)$$

In the equations above,

\bar{x} is the field point,

$\bar{\zeta}$ is the source point, and

c is some constant used to normalized the two dimensional Green's function which has an important effect on the stability criteria of the numerical scheme.

The Green's functions G and G^* are both solutions of Poisson equation. G^* has an arbitrary constant $\ln c$, which will be important in the stability criteria of the numerical scheme. Substituting eqs. (13 -16) into eq. (12), new surface integral equation for the potential ϕ of the point \bar{x} in domain V is produced. The Velocity potential in two dimensions is expressed as:

$$\phi(\bar{x}; t) = - \int \left(\phi \frac{\partial G}{\partial n} - G \frac{\partial \phi}{\partial n} \right) dl = -\frac{1}{2\pi} \int \left\{ \phi(\bar{\zeta}, t) \frac{\bar{n}(\bar{\zeta}) \cdot (\bar{x} - \bar{\zeta})}{|\bar{x} - \bar{\zeta}|^2} + \frac{\partial \phi}{\partial n}(\bar{\zeta}, t) \ln |\bar{x} - \bar{\zeta}| \right\} dl. \quad (17)$$

If G^* instead of G is used in the integral equation, then,

$$\phi(\bar{x}; t) = - \int \left(\phi \frac{\partial G^*}{\partial n} - G^* \frac{\partial \phi}{\partial n} \right) dl = -\frac{1}{2\pi} \int \left\{ \phi(\bar{\zeta}, t) \frac{\bar{n}(\bar{\zeta}) \cdot (\bar{x} - \bar{\zeta})}{|\bar{x} - \bar{\zeta}|^2} + \frac{\partial \phi}{\partial n}(\bar{\zeta}, t) \ln c |\bar{x} - \bar{\zeta}| \right\} dl. \quad (18)$$

As \bar{x} approaches the boundary, the potential value on the boundary is derived in a principal value integral form such as,

$$\phi(\bar{x}, t) = -\frac{1}{\pi} \int \left\{ \phi(\bar{\zeta}, t) \frac{\bar{n}(\bar{\zeta}) \cdot (\bar{x} - \bar{\zeta})}{|\bar{x} - \bar{\zeta}|^2} + \frac{\partial \phi}{\partial n}(\bar{\zeta}, t) \ln |\bar{x} - \bar{\zeta}| \right\} dl, \quad (19)$$

$$\phi(\bar{x}, t) = -\frac{1}{\pi} \int \left\{ \phi(\bar{\zeta}, t) \frac{\bar{n}(\bar{\zeta}) \cdot (\bar{x} - \bar{\zeta})}{|\bar{x} - \bar{\zeta}|^2} + \frac{\partial \phi}{\partial n}(\bar{\zeta}, t) \ln c |\bar{x} - \bar{\zeta}| \right\} dl. \quad (20)$$

Where, \bar{x} and $\bar{\zeta} \in S$ and \bar{n} is an outward unit normal vector.

This equation shows that the velocity potential ϕ at (\bar{x}, t) can be expressed in terms of the boundary values only, without any information from inside the volume. In other words, the BIM reduces the space dimension by one, which is the essential benefit of the BIM. For the free surface problem, this method is adequate since the physical values of interest are usually only on the boundaries.

4. The time stepping schemes

Once Laplace's equation is solved in the fluid domain, the normal derivatives of the potentials on the free surface and the potentials on the body surface being obtained. With this information, the kinematics and the dynamic free surface boundary conditions determine the new location of the free surface for the next time step and estimate the potential on the new free surface. The new location and the new potential on the new location are used as a boundary condition of stage (1), and the result of stage (1) is used for the next stage, and so on.

The following notations are adopted.

- Δt is the time increment,
- η^n, η^{n+1} is the free surface location at time intervals t^n and t^{n+1} new time level,
- ϕ^n, ϕ^{n+1} is the velocity potential at both time levels t^n and t^{n+1} , respectively, and
- ϕ_n^n is the normal derivative of the velocity potential ϕ^n at time level t^n .

Using the above notations, the fourth order Runge Kutta method is expressed as,

$$\phi^{n+1} = \phi^n + \frac{1}{6}(k_1 + 2k_2 + 2k_3 + k_4), \quad (21)$$

and

$$\eta^{n+1} = \eta^n + \frac{1}{6}(l_1 + 2l_2 + 2l_3 + l_4). \quad (22)$$

Where, k_i and l_i are the intermediate increments of ϕ and η , respectively. Using the explicit scheme, all the intermediate $d\phi$ (such as k_1, k_2, k_3 or k_4) and $d\eta$ (such as K_1, K_2, K_3 , or K_4) are calculated from the previous values. The increments k_1 and l_1 are calculated from the values of the (n) step. k_2 and l_2 are calculated from the

values of k_1 and l_1 intermediate step, and so on in a similar fashion for k_3 and l_3 , and k_4 and l_4 . Details of such increments can be found in standard numerical analyses textbook.

5. Solution of the boundary value problem

To apply the free surface boundary condition in the Lagrangian step of the two-stage method, the unknown ϕ_n^n on the free surface is calculated using the Boundary Integral Method (BIM). The BIM starts with Green's second identity and results in an integral equation for the potential on the boundary. The potential $\phi(\vec{x})$ of the domain V is depicted as;

$$\phi(\vec{x}) = - \int \left(\phi \frac{\partial G}{\partial n} - G \frac{\partial \phi}{\partial n} \right) dl. \quad (23)$$

Where G is the Green's function of equation (14). Discretizing the surface with line segments, the potential ϕ at the (i^{th}) segment is approximated as:

$$\phi_i(\vec{x}) = - \sum \left\{ \phi_j \int_{\Delta x_j} \frac{\partial G_{ij}}{\partial n_j} dl_j - \left(\frac{\partial \phi}{\partial n} \right)_j \int_{\Delta x_j} G_{ij} dl_j \right\}. \quad (24)$$

Where,

ϕ_j is known on the free surface, and

$\frac{\partial \phi_j}{\partial n_j}$ is unknown on the free surface.

Either ϕ_j or $\left(\frac{\partial \phi}{\partial n} \right)_j$ is known and the other

one is unknown on the remaining surfaces S_B and S_{bottom} .

6. Pressure calculation

As the body starts to move from rest, the body experiences a changing hydrodynamic force imposed on it. The fluid forces are

estimated by the pressure integration over the wetted surface. An exact force prediction leads to reliable structural analysis for safe design of ship structures.

The equation for the pressure calculation on the body is derived from Bernoulli's equation for inviscid, incompressible, and irrotational flow.

$$\frac{P}{\rho} = -\frac{\partial\phi}{\partial t} - \frac{1}{2} \nabla\phi \cdot \nabla\phi - gy$$

$$= -\frac{d\phi}{dt} + \bar{U} \cdot \nabla\phi - \frac{1}{2} \nabla\phi \cdot \nabla\phi - gy \quad (25)$$

Where,

\bar{U} is the velocity of the body, and $\nabla\phi$ is the velocity of the particle.

This equation consists of three parts:

1. the unsteady time varying pressure component, $\frac{\partial\phi}{\partial t}$,
2. the dynamic pressure component with the nonlinear term, $\bar{U} \cdot \nabla\phi - 0.5\nabla\phi \cdot \nabla\phi$, and
3. the static pressure term which is proportional to the depth, $-gy$.

On the body, the normal derivative of $\frac{d\phi}{dt}$ is derived using rigid dynamics and a vector identity,

$$\frac{d}{dt} \left(\frac{\partial\phi}{\partial n} \right) = \frac{d}{dt} (\bar{n} \cdot \nabla\phi)$$

$$= \bar{n} \cdot \frac{d}{dt} \nabla\phi + \nabla\phi \cdot \frac{d\bar{n}}{dt}$$

$$= \bar{n} \cdot \left(\frac{\partial}{\partial t} \nabla\phi + (\bar{U} \cdot \nabla) \nabla\phi \right) + \nabla\phi \cdot (\bar{\omega} \times \bar{n})$$

$$= \bar{n} \cdot \left(\nabla \frac{\partial\phi}{\partial t} + \nabla(\bar{U} \cdot \nabla\phi) + \bar{\omega} \times \nabla\phi \right) + \nabla\phi \cdot (\bar{\omega} \times \bar{n}), \quad (26)$$

where; $\bar{\omega}$ is the rotational velocity of the body.

Since $\bar{U} \cdot \nabla\phi$ and $\frac{d\phi}{dt}$ satisfy Laplace's equation. With Laplace's equation and the various boundary conditions, the boundary

value problem is solved for $\frac{d\phi}{dt}$ on the body

and $\frac{\partial}{\partial n} \left(\frac{d\phi}{dt} \right)$ on the free surface. Once $\frac{d\phi}{dt}$ on

the body is obtained, the pressure on the body is calculated with eq. (25).

The slamming force on the body can be obtained by direct integration of the pressure distribution over the wetted surface of the body. This force can be determined using the definition of added mass and conservation of vertical momentum as;

$$F(t) = \frac{d}{dt} (M_a U), \quad (27)$$

where, M_a is the infinite frequency added mass in heave for the submerged portion of the body, which can be calculated by the commonly used form [24].

$$M_a = C_a Y^2 \text{ and } C_a = (1 - \alpha/2\pi)^2 \pi/2. \quad (28)$$

With α is the deadrise angle of the wedge surface and Y is the depth of the wetted part of the wedge, fig. 2.

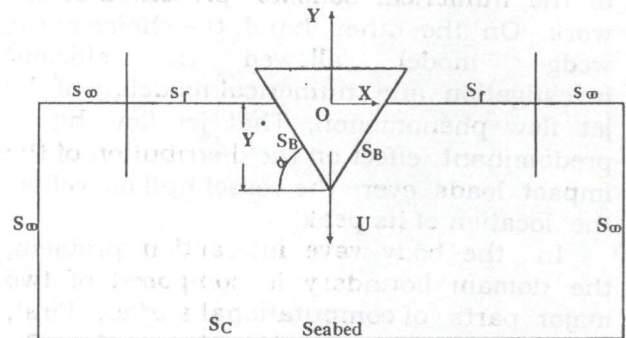


Fig. 2. The body geometry and the coordinate system for the wedge section.

The instantaneous velocity of the wedge during the impact is given by;

$$V(t) = \frac{V_0}{1 + M_a / M}, \quad (29)$$

where,

V_0 is the falling velocity of the body at initial

impact ,
 M is the mass of the body, and
 M_a is the infinite frequency added mass in
 heave as mentioned above.

7. Discussion and application to wedges

Although, the present method is valid for an arbitrary shaped body sections, the wedge section was selected as a case study. The body geometry and the coordinate system for the wedge section is illustrated in fig. 2. It is worth mentioning that the wedge model chosen in the present work is considered as the prototype shape for transverse sections of the fast vessels, that are subjected to slamming forces resulted from their proposing motion. The wedge section is the standard element in the structural construction of high-speed vessels especially with varying deadrise angle. Furthermore, the wedge shaped section represents the bow section of a ship, that section is mostly subjected to that type of impact forces along the longitudinal axis of the ship. Moreover, the availability of experimental results related to the chosen wedge model allowed the verification of the accuracy and efficiency of the numerical scheme presented in this work. On the other hand, the choice of the wedge model allowed the efficient investigation and numerical modeling of the jet flow phenomenon. That jet flow has a predominant effect on the distribution of the impact loads over the vessel hull as well as the location of its peak.

In the body-wave interaction problem, the domain boundary is composed of two major parts of computational surface. First, the body surface S_B and the free surface S_f (figs. 1 and 2), and these two surfaces meet in one line. This line referred to as the intersection point for the case of two-dimension study. In a simplified mathematical model, the intersection point is represented as having a sharp corner, which induces a jump in the physical value and introduces singularities in the mathematical calculations. The problem arises because of the need to satisfy two boundary conditions at this point, namely the body boundary

condition and the free surface boundary condition. To eliminate these singularities, a special treatment of the velocities at that point is needed. The tangential velocity component at the intersection point was determined by the modified Lagrangian polynomials interpolation scheme. While, the normal velocity component is determined by the body boundary that is to be the same as the normal velocity of the body.

Since the length of the wetted surface varies during the motion and is deepened on the deadrise angle, hence it has been normalized for plotting conveniences. So, the wetted body surface is subdivided to two regions. The first region represented by the normalized distance from (-1 to 0), namely the submerged portion of the model. The second region is represented by the normalized distance form (0 to 1), namely the portion of the model located above the calm water surface. For verification purposes, both numerical results, obtained using the present numerical scheme and corresponding experimental data form [26, 27] are plotted.

The pressure distributions on the wetted surface of the model with different deadrise angles are shown in figs. 3 to 6. It can be noticed that, over the first region, good agreement between the numerical results and corresponding available experimental data does exist for all ranges of the deadrise angles. From these figures it is apparent that, almost constant pressure distribution is experienced over that region, with slightly varying gradient as the deadrise angle increases. From physical point of view the static component of the pressure, eq. (25), is predominant on that region. Hence, this explains the direct proportional relation between the value of the deadrise angle and the gradient of the pressure distribution over that region. Furthermore, the dynamic effect of the pressure component is mainly manifested on the magnitude of the pressure rather than the variations of the pressure gradient. This is noticed from the figures where higher values of pressure are obtained with smaller deadrise angle, and vice versa.

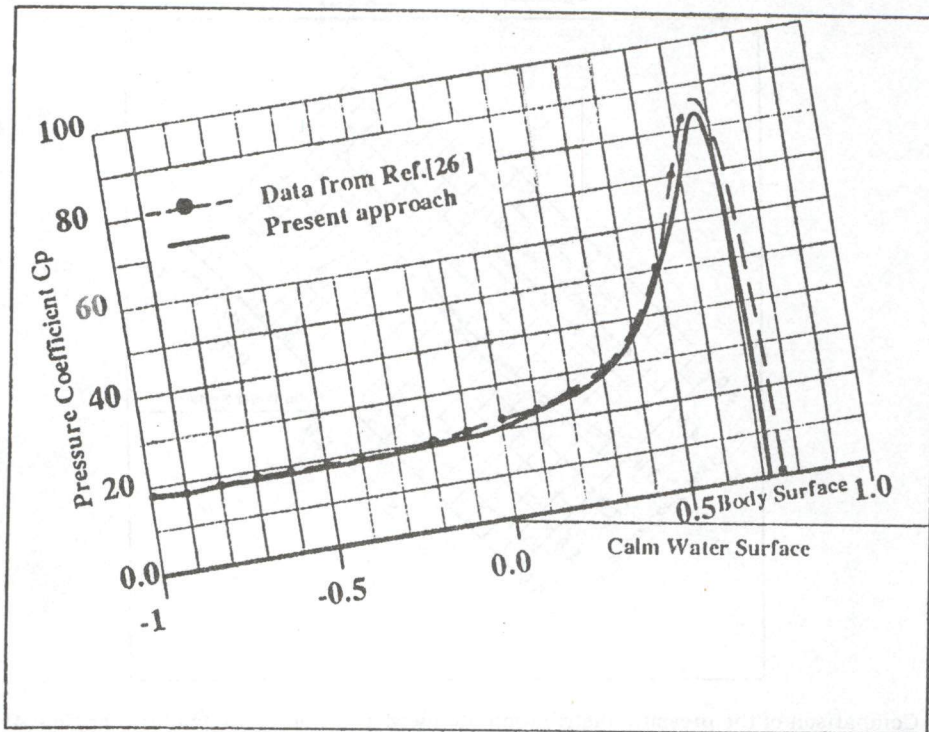


Fig. 3. Comparison of the pressure distribution on a wedge surface with deadrise angle = 10 degrees.

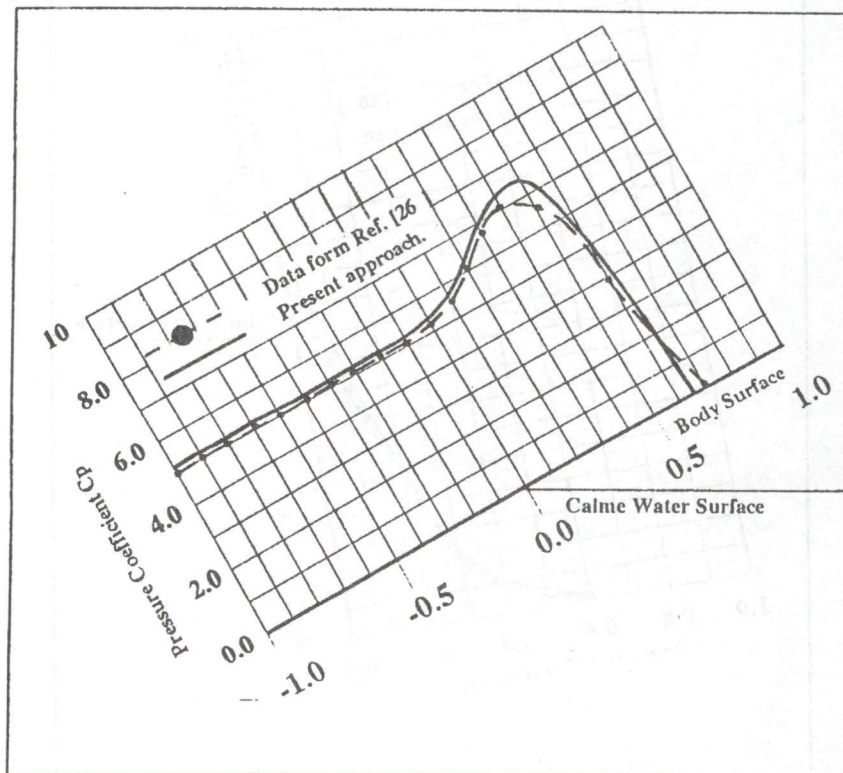


Fig. 4. Comparison of the pressure distribution on a wedge surface with dead rise angle = 30 degrees.

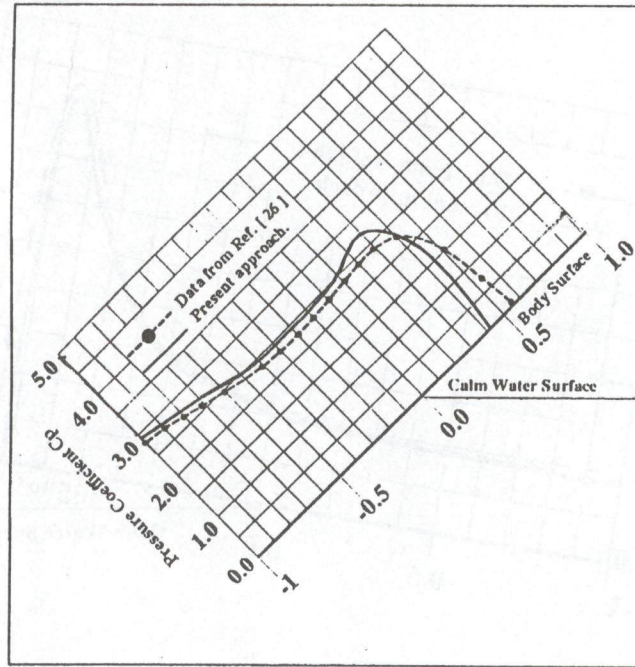


Fig. 5. Comparison of the pressure distribution on a wedge surface with dead rise angle = 45 degrees.

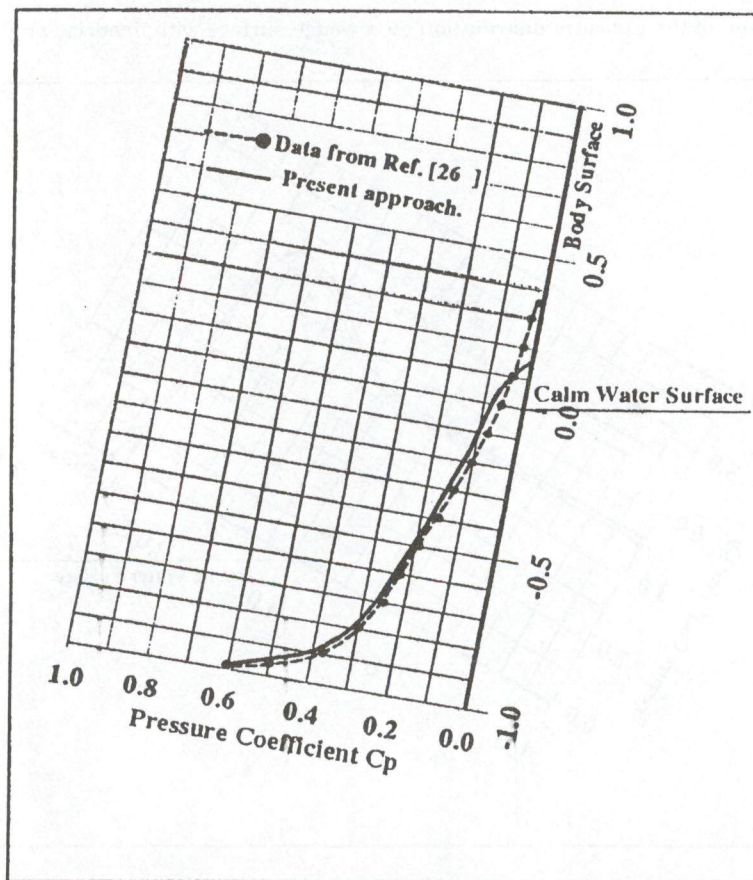


Fig. 6. Comparison of the pressure distribution on a wedge surface with dead rise angle = 80 degrees.

Moreover, for higher values of deadrise angle the maximum pressure magnitude is concentrated at the keel point as shown in fig. 6.

On the other hand, the second region of the model is mainly affected by the free surface configuration. The jet effect causes the pressure distribution to exhibit a noticeable increase in pressure magnitude especially for smaller values of deadrise angle. This is probably due to the impact load of the jet with the body surface. The noticed hump in the pressure distribution decreases with increase in deadrise angle. This can be explained by the fact that with increasing deadrise angle the jet flow leaves the wedge surface tangentially upwards and hence the pressure gradient along the body surface in this region falls rapidly. Noticeable differences between the numerical results obtained and the available experimental data exist in that region. As might be expected, very severe difficulties are encountered when the deadrise angle has a large value, because of the fast moving jet flow as shown in fig. 6. This is due to the lack of exact mathematical formulation in modeling the jet resolution, and hence poor numerical simulation in that region. This issue is a difficult one to address due to the sensitivity of the jet profile and its formation.

In order to demonstrate the capability of the present method in resolving the phenomenon of the jet flow, the influence of the decreasing angle on the jet formation is investigated. Fig. 7 shows the flow for a wedge with deadrise angle ($\alpha=60$ degree) entering the fluid with high speed. For high speeds of entry it is reasonable to expect self-similarity since locally near the wedge the fluid particle acceleration will be much greater than gravity, especially in the early stages of entry. Starting from the initial conditions with just the wedge vertex in calm water, the free surface quickly becomes self-similar and compares well with the results of Dobrovolskys [26]. While in the jet region, the fluid particles move slightly further up the wedge surface and will behave approximately as a free projectiles moving under gravity alone. So, the real simulation would be further complicated. This

instability would eventually preclude further time stepping of the solution. A remarkable difference can be shown in fig. 7. This disagreement with the results of Dobrovolskaya [26] in that region, certainly indicates a weakness in the present scheme, probably associated with poor numerical resolution of the jet.

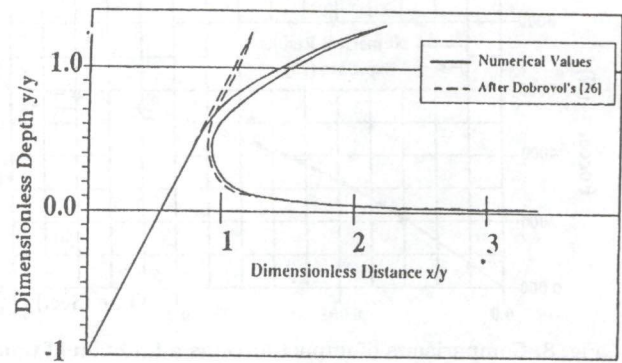


Fig. 7. Comparison of the jet flow on a wedge surface with deadrise angle = 60 degrees.

The impact force as a function of time on the wedge surface is also compared with the experimental data of Zhao [25] for the wedge with deadrise angle (30 degree) fig. 8. The numerical values show a good agreement with the experimental ones especially at the beginning of the motion and moderate values of time. As the jet flow starts to be the predominant behavior of the flow, higher values of time, a remarkable difference can be shown which is related to the poor numerical simulation of the jet flow. For the reason to examine the effect of deadrise angle on the impact force over the body surface, the force coefficient is plotted as a function of the deadrise angle as shown in fig. 9. The force coefficient is defined as,

$$C_F = \frac{F}{\rho v^2 y^*}$$

Where,

v is the wedge entry velocity, and

y^* is the depth of the wedge vertex.

As might be expected, the inverse relation between values of the force coefficient and the deadrise angle is quite

clear as shown in fig. 9. The variation in the gradient of this function from a limited slope over the region of small deadrise angle to a sever slope over the region of moderate and high deadrise angles, reveals that, the activity of the jet flow is proportional to the value of the deadrise angle.

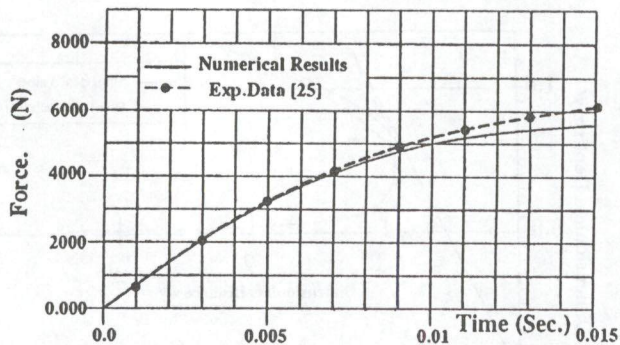


Fig. 8. Comparisons of impact force as a function of time for wedge with deadrise angle 30 degrees.

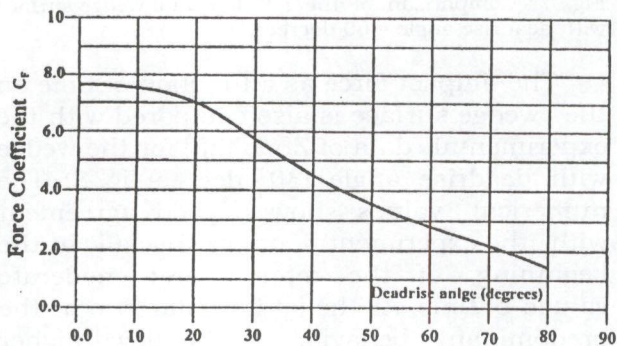


Fig. 9. Forces coefficient as a function of deadrise angle for wedge shape.

8. Conclusions

The proposed approach is readily capable to handle time-dependent free surface flows with fully non-linear free surface boundary conditions and arbitrarily shaped heaving body geometry. The model satisfied the boundary conditions on the exact instantaneous position of the moving body and the free surface. The captive mode was tested by water entry of symmetric wedges in a gravity field. Pressure distributions were calculated at different deadrise angles as well as the impact force. Moreover the computational procedure has been tested by comparison for the detailed sensitivity

performed on jet flow phenomenon. However, the difficulties in resolving the jet flow numerically must be recognized, since its position and profile are very sensitive.

References

- [1] T. Von Karman, "The Impact of Seaplane Floats During Landing" NACA, TN 321, Washington (1929).
- [2] H. Wagner, "The Phenomena of Impact and Planning on water" NACA [Translation 1366] Math. Mech, Vol. 12 (4), pp. 193-215 (1932).
- [3] Yu, Y.S, and F. Ursell, "Surface Waves Generated by an Oscillating Circular Cylinder on Water of Finite Depth: Theory and Experiment". J. Fluid Mech, Vol. 11, pp. 529-551 (1961).
- [4] A. Papanikol. and H. Nowacki, "Second Order Theory of Oscillating Cylinders in a Regular Wave," Proceedings 13th Symposium on Naval Hydrodynamics, Tokoy (1980).
- [5] T. Inje, and P. Brevig, "Non-Linear Ship Motions" in Proceedings, third international Conference on Numerical Ship Hydrodynamics, Paris, June (1981).
- [6] Greenhow, M and Lin, W.M., "Nonlinear Free Surface effects: Experiments and Theory," Department Ocean Engineering Report (83-19), Massachusetts Institute of Technology. Cambridge Mass. (1983).
- [7] C.M. Lee, "The Second-Order Theory of Heaving Cylinders in a Free Surface" J. Ship Research, Vol. 12 (4) (1968).
- [8] R.B. Chapman. "Large Amplitude Transient Motion of Two-Dimensional Floating Bodies" J. Ship Research, Vol. 23 (1), pp. 20-31 (1979).
- [9] M. Greenhow, "Wedge Entry Into Initially Calm Water" Applied Ocean Research, Vol. 9 (4) (1987).
- [10] D.G. Dommermuth and D.K. Yue "Numerical Simulations of Nonlinear Axi-Symmetric Flows With a Free Surface" J. Fluid Mech, Vol. 178, pp. 195-219 (1987).
- [11] Pukhnachoy and A.A. Korobkin "Initial Stage of Water Impact" Ann. Rev. Fluid Mech, Vol. 20, pp. 159-185 (1988).

- [12] S.D. Howison K.S. Wilson "Incompressible Water entry problems at small Deadrise Angles" *J. Fluid Mech*, Vol. 22, pp.215-230 (1991).
- [13] N. Kolluru Venkat. and M.L. Spaulding. "Numerical Simulation of Nonlinear Free Surface Flow Generated by a Heaving Body of Arbitrary Cross-Section" *J. Ship Research*, Vol. 34 (2), pp. 92-104 (1990).
- [14] T.S. Angell, G.C. Hsiao. "An Integral Equation for the Floating Body Problem" *J. Fluid Mech*. Vol.166, pp.161-171 (1986).
- [15] G. Reenhow, M and Lin,W.M "Numerical Simulation of Free Surface Flows Generated by Wedge Entry and Wave Maker Motion," *Proceeding 4th International Conference on Numerical Ship Hydrodynamics*, National Academy of Sciences, Washington ,D.C, pp. 94-106 (1985).
- [16] D. SEN, J.S. Oawlowski, J. Lever, and M.J. Hinchey "Two-Dimensional Numerical Modeling of Large Motions of Floating Bodies in Waves, *Proceedings, 5th International Conference Numerical Ship Hydrodynamics*, Hiroshima, pp. 257-277 (1989).
- [17] D. SEN, "Numerical Simulation of Motions of Two-dimensional floating Bodies " *J. ship Research*, Vol. 37 (4), pp. 307-330 (1993).
- [18] X.M. Wang and M.L. Spaulding "A two Dimensional Potential Flow Model of the Wave Field Generated by a Semisubmerged Body in Heaving Motion" *J.Ship Research*, Vol. 32 (2), pp. 83-91 (1988).
- [19] Xiaoming Mei,Yuming Liu, Dick K.P.Yue "On the Water Impact of General two-Dimensional Sectios" *Applied Ocean Research*, Vol. 21, pp. 1-15 (1999).
- [20] Kharif and Ramamonjariisoa,"On the Stability of Gravity Waves on Deep Water", *J. Fluid. Mech*, Vol. 218, pp. 163-170 (1990).
- [21] S. Christiansen "A stability Analysis of a Eulerrian Solution Method for Moving Boundary Problems" *J. Comp. Appl. Math.*, Vol. 33, pp. 269-296 (1990).
- [22] B. Alexander Stavovy and Shen-Lun Chuang "Analytical Determination of Slamming Pressure for High-Speed Vehicles in Waves" *J.Ship Research*, Vol. 20 (4), pp190-198 (1976).
- [23] G.X.Wu "Anote on Non-Linear Hydrodynamic Force on a Floating Body" *Applied Ocean Research*, Vol. 22, pp. 315-316 (2000).
- [24] R. Zhao O. Faltinsen "Water Entry of Two-Dimensional bodies" *J. Fluid Mech.*; Vol. 24, pp. 593-612 (1993).
- [25] R. Zhao, O. Faltinsen J. Arnsnes "water Entry of an Arbitrary Two-Dimensional Section with and Without Flow Separation" *ONR, Norway* (1996).
- [26] Z. Dobrovol'skaya. "On Some Problems of Singularity Flow of a Fluid with a Free Surface" *J.Fluid Mech*, Vol. 36(4), p. 805 (1969).
- [27] D.G. Dommermuth, and Yue, D.K.P, LIN,W.m, Rapp, R.J and Melville."A Comparison Between Potential Theory and Experiments" *J. Fluid Mech*, Vol. 189, pp. 423-442 (1988).
- [28] S.K Wilson. "Incompressible Water Entry Problems at Small Deadrise Angles" *J. Fluid Mech*, Vol. 222, pp. 215-230 (1991).

Received December 26,2001

Accepted January 19,2002

1947
1948
1949
1950
1951
1952
1953
1954
1955
1956
1957
1958
1959
1960
1961
1962
1963
1964
1965
1966
1967
1968
1969
1970
1971
1972
1973
1974
1975
1976
1977
1978
1979
1980
1981
1982
1983
1984
1985
1986
1987
1988
1989
1990
1991
1992
1993
1994
1995
1996
1997
1998
1999
2000
2001
2002
2003
2004
2005
2006
2007
2008
2009
2010
2011
2012
2013
2014
2015
2016
2017
2018
2019
2020
2021
2022
2023
2024
2025

1947
1948
1949
1950
1951
1952
1953
1954
1955
1956
1957
1958
1959
1960
1961
1962
1963
1964
1965
1966
1967
1968
1969
1970
1971
1972
1973
1974
1975
1976
1977
1978
1979
1980
1981
1982
1983
1984
1985
1986
1987
1988
1989
1990
1991
1992
1993
1994
1995
1996
1997
1998
1999
2000
2001
2002
2003
2004
2005
2006
2007
2008
2009
2010
2011
2012
2013
2014
2015
2016
2017
2018
2019
2020
2021
2022
2023
2024
2025